2-amino -5-chloropyridinium-trichloroacetate[22], 2-amino -5-chloropyridinium-4hydroxybenzoate[23], 2-amino -5-chloropyridinium-benzoicacid[24], 2-amino-5-chloro-pyridinium-L-tartrate[25] have been reported as a potential candidate for chemical, industrial and medical applications. In this family, the structure of 2-amino-5-chloropyridinium trifluoroacetate is already reported by (Madhukar Hemamalini and Hoong-kun fun in 2010). As there is lack of information on the material's growth aspects and testing the quality for the possibility of device fabrications, the present work attempts are made to grow 2-amino-5-chloropyridinium-trifluoroacetate crystal by slow evaporation technique using methanol as a solvent. The successfully obtained crystal property was analysed by single-crystal X-ray diffraction, spectral, optical, thermal, dielectric, laser damage threshold and powder SHG studies.

2 Experimental section

2.1 Materials synthesis and crystal growth

The 2A5CTFA crystal was synthesised by combining 2-amino-5-chloropyridine (Avra 98%) with trifluoroacetate acid (Avra 98%) in 1:1 molar ratio with methanol as the solvent. Fig. 1 depicts the chemical procedure used to achieve the 2-amino-5-chloropyridinium trifluoroacetate compound. The appropriate quantity of 2-amino-5-chloropyridine was initially dissolved in the desired quantity of methanol and then trifluoroaceticacid was gradually added to the 2-amino-5-chloropyridine solution while stirring gently. The homogeneous mixture of the solution was attained by stirring the solution for about 6 hours with a magnetic stirrer. To eliminate the suspended contaminants, the resulting solution was filtered using high-quality filter paper. The beaker containing the filtered solution was covered with a thin polythene sheet with fine holes to have the controlled solvent evaporation. The continous slow evaporation process of the filtered solution kept in a dust-free environment initiate the nucleation of crystallization. Good quality seed crystal obtained during crystallization was suspended in the mother solution for further evaporation, yield crystals of size 12 × 7.5 × 1.8 mm^3 within a period of 18 days. The photograph of the as grown single crystal is shown in Fig. 2.

3 Methods of characterization

The grown single crystal was investigated by various characterization techniques to access its feasibility for device fabrications. The structural property of the crystal is investigated by using the BRUKER KAPPA APEX II CCD single crystal X-ray diffractometer using the MoKα radiation (λ=0.71 Å) at ambient temperature. The functional groups of the crystal are identified by using the spectroscopic techniques such as FT-IR (1.0 cm^{-1}) and FT-RAMAN (2.0 cm^{-1} resolution) in the wavenumber range of 4000-400 cm^{-1}.and 4000-50 cm^{-1} respectively. The UV-Visible-NIR spectrum was recorded by Perkin Elmer LAMBDA 950 Spectrophotometer in the wavelength region of 200-1100 nm. The thermal stability of 2A5CTFA was determined by the TG-DTA analysis with the help of NETZSCH STA 449 F3 simultaneous thermal analyser in nitrogen atmosphere at the temperature range 50-900 °C. The PL emission property of the crystal was analysed using Fluorocube (Jobin-Vyon M/S) spectro-fluorometer. The dielectric behaviour of the crystal

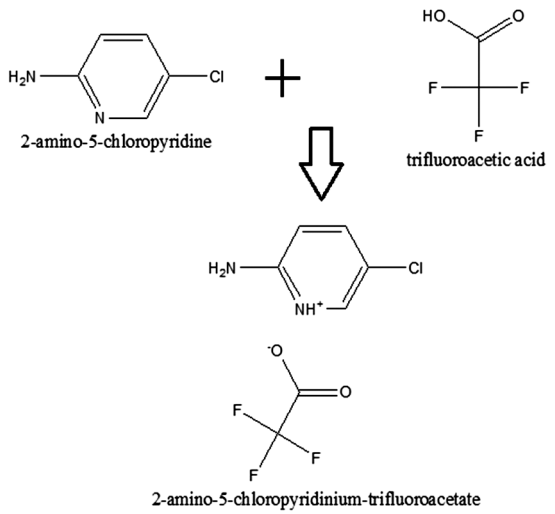

Fig. 1 — Reaction scheme of 2A5CTFA in methanol

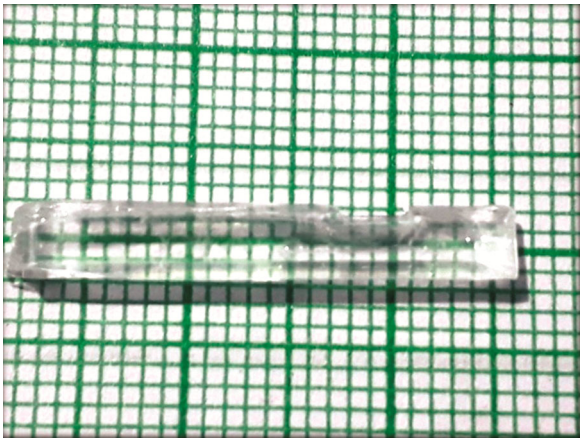

Fig. 2 — Photograph of as grown single crystal of 2A5CTFA

Table 1 — FTIR and FT-RAMAN band assignments of 2A5CTFA

FTIR spectrum (cm^{-1})	FT-RAMA spectrum (cm^{-1})	Assignments
3254	-	NH stretching vibration of primary amine
3075, 3033	3083, 3055	C - H stretching vibration of pyridinium ring
2763	-	O - H stretching vibration
1630	1631	C = C stretching vibration
1678	1676	C = O asymmetric stretching vibration of TFA
1547	1547	N – H bending vibration of primary amine
1433	1434	C = O symmetric stretching vibration of TFA
1344	1324, 1349	NO_2 symmetric stretching vibration
1205	-	CF_3 stretching vibration
1254	1253	C – N stretching vibration
1182, 1132, 911	1158	NH2 Rocking and out of plane bending modes
1001	-	CH in plane bending
851, 832	795, 850	CH out of plane bending
722	-	CH_2 rocking vibration
514	-	NO_2 rocking vibration

Fig. 4 — UV-Visible transmission spectrum of 2A5CTFA crystal

FT-Raman spectrum.

C-H Vibrations

The C-H stretching vibration of aromatic ring peak noted at 3075, 3033 cm^{-1} in FT-IR and at 3083, 3055 cm^{-1} in FT-Raman spectrum. The peak observed at 1001 cm^{-1} in FT-IR spectrum corresponds to C-H in-plane bending vibration and the peak noted at 851, 832 cm^{-1} in FT-IR and at 795, 850 cm^{-1} in FT-Raman spectrum corresponds to C-H out-of-plane bending vibration.

CH_2 and CF_3 Vibrations

The CH_2 rocking vibration peak observed at 722 cm^{-1} in FT-IR spectrum. The CF_3 stretching vibration peak observed at 1205 cm^{-1} in FT-IR spectrum.

C=O, C=C and C=N Vibrations

The peaks observed at 1678 cm^{-1} in FT-IR and 1676 cm^{-1} in Raman spectrum is due to the asymmetric stretching of C=O and the symmetric stretching vibration of C=O group is observed at 1433 cm^{-1} in FT-IR and 1434 cm^{-1} in Raman spectrum. The stretching vibration peak of C=C group is noticed at 1630 cm^{-1} in FT-IR and 1631 cm^{-1} in Raman spectrum. The peak noted at 1483 cm^{-1} corresponds to the C=N stretching vibration in FT-IR and at 1487 cm^{-1} in FT-Raman spectrum. The C=N stretching of primary amine is observed at 1183 cm^{-1} in FT-IR spectrum.

O-H and C-N Vibrations

The O-H out-of-plane bending vibration peak was noticed at 911 cm^{-1} and stretching modes of OH vibration peak observed at 2763 cm^{-1} in the FT-IR spectrum. The stretching vibration peak of C-N group observed at 1254 cm^{-1} in FT-IR and at 1253 cm^{-1} in FT-Raman spectrum respectively.

NO_2 Vibrations

The NO_2 symmetric stretching vibration peak was observed at 1344 cm^{-1} in FT-IR and at 1324, 1349 cm^{-1} in FT-Raman spectrum. The NO_2 group rocking vibration peak is observed at 514 cm^{-1} in FT-IR spectrum. The significant Infrared and Raman respective wavenumbers and their equivalent frequency assignments are given in Table 1.

4.3 Optical absorption studies

A good NLO crystal must possess efficient optical transparency and a cut-off wavelength below 400 nm[27]. In such an aspect, the absorption/transmission spectrum is essential to extract valuable information concerning the electronic transitions, transparency, and the optical band gap[28]. The optical transmission spectrum of the grown single crystal is obtained between 200-1000 nm

spectral region and depicted in Fig. 4. Examination of the spectrum shows 85 percent transmittance in the 400-1000 nm spectral range with a cut-off wavelength at 345 nm. The higher transmittance in the visible and near IR region is due to the existence of a delocalized electron cloud in the molecule and is a desirable parameter for materials possessing NLO property. The absorption coefficient (α) is calculated by using the relation[29]

$$\alpha = \frac{2.303\left(\frac{1}{T}\right)}{t} \quad \ldots (1)$$

Where, 'T' is the transmittance and 't' is the thickness of the 2A5CTFA crystal.

The optical band gap (E_g) of the crystal is estimated using the tauc's equation,

$$(\alpha h\nu) = A\left(E_g - h\nu\right)^n \quad \ldots (2)$$

Where, h is the Planck's constant, ν is the frequency of incident radiation and A is a constant. The numerical value of exponent n in equation 2 indicates different types of transition process namely, direct allowed transition (n = ½), indirect allowed transition (n = 2), direct forbidden transition (n = 3/2) and indirect forbidden transition (n = 3)[30]. As the material has direct allowed transition, to determine the band gap the Tauc plot represented by Fig. 5 is drawn between the photon energy (hν) along the x-axis and $(\alpha h\nu)^2$ along the y-axis. The extrapolation of the linear portion of the plot towards x-axis, gives the optical bandgap of the crystal, which is found to be 3.54 eV. Theoretically, the optical bandgap value was calculated using the equation $E = \frac{hc}{\lambda}$ where 'h' is the Planck's constant (6.626×10^{-34}Js) and 'λ' is the absorption edge wavelength of the crystal. The optical bandgap calculated theoretically was found to be 3.59 eV, and it agress well with the experimental band gap value. Hence, the grown 2A5CTFA crystal with excellent transparency in the Vis-near IR region, lower cut-off wavelength and a wide bandgap of 3.54 eV make them a potential candidate in photonics and optoelectronic devices.

4.4 Thermal analysis

The TG-DTA analysis was carried out using a NETZSCH STA 449F3 thermal analyser in nitrogen environment at a heating rate of 10 K/min upto 400 °C starting from room temperature using an alumina crucible to study the thermal stability of the grown-up 2A5CTFA crystal. This study was performed on a 2.64 mg powdered sample and the thermograph obtained is shown in Fig. 6. Thermogravimetric curve reveals that the 2A5CTFA crystal was thermally stable up to 137 °C, signifying that there is no decomposition or phase transition occurred upto this temperature. The preliminary weight loss of the crystal starts from the temperature of 137 °C to 178 °C. Furthermore, in the title compound 2-Amino-5-Chloropyridinium trifluoroacetate crystal the significant weight loss of 98.12 percent was found to be from 178 °C to 217.83 °C and it is due to the liberation of CO_2, H and O molecules[31-32]. Finally, the material completely decomposed between 217.83 °C and 352.8 °C with a mass change of 2.86 percent. The sharp endothermic peak on the DTA curve detected at 207 °C corresponds to the melting temperature of 2A5CTFA crystal. It is also noticed that after 224.02 °C the decomposition of the material is observed to be gradual. Therefore from the aforesaid results, it can be inferred that the 2-amino-5-chloropyridinium-

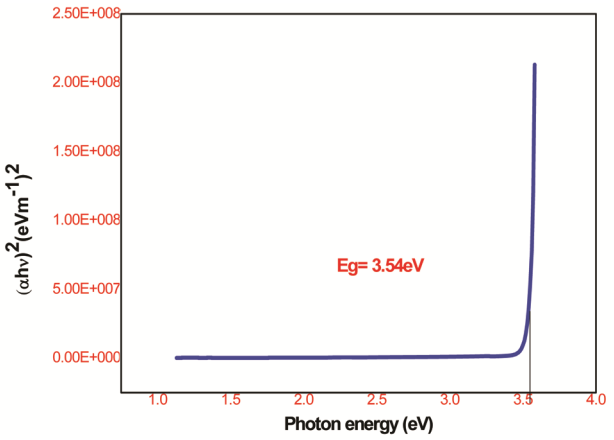

Fig. 5 — Tauc plot of 2A5CTFA crystal

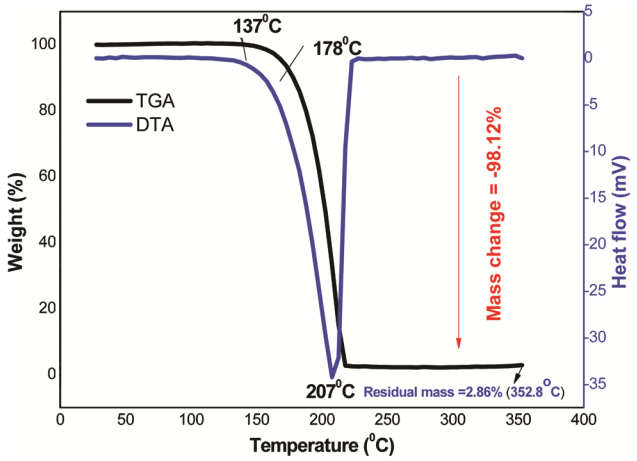

Fig. 6 — TG-DTA thermal profile of 2A5CTFA single crystal

Table 2 — Comparison of 2A5CTFA thermal stability with other nonlinear optical crystals

Compounds	Thermal stability (℃)	Reference
2-(4-Fluorobenzylidene) malononitrile	119.81	[33]
Anilinium D-tartrate	132.5	[34]
Guanidiniummanganese sulphate hydrate	73	[35]
4CALTM	85	[36]
LAT	118	[37]
2-Amino-5-chloropyridinium-2,4-dinitrophenolate	122	[38]
2-Amino-5-chloropyridine	109.85	[39]
2-amino 5-chloropyridinium 4-carboxybutanoate	119	[40]
2-Amino-5-chloropyridinium-trifluoroacetate	137	Present work

trifluoroacetate crystal can be used effectively to fabricate photonic devices at the temperature below 137 °C. The comparison of the thermal stability of 2A5CTFA crystal with other important organic crystal is presented in Table 2.

4.5 Laser-induced damage threshold study

The efficient crystal not only relies on nonlinear optical properties, but also depends on its surface quality to uphold high intensity laser light[41]. The laser damage threshold value is the most significant parameter to use the materials towards device fabrications[42-44]. A laser damage threshold investigation for 2A5CTFA crystal was analysed using a 1064 nm Q-switched Nd: YAG laser operating in QUANTA RAY mode with a pulse width of 6 ns and a recurrence rate of 10 Hz. The LDT value of 2-Amino-5-Chloropyridinium trifluoroacetate was estimated by using the formula,

$$\text{Power density } (P_d) = \frac{E}{\tau \pi r^2} \text{ (GW/cm}^2\text{)} \quad \ldots (3)$$

In the equation, 'E' is the peak value of input energy (mJ), 'τ' is the pulse width (ns) and 'r' is the area of the circular spot (mm). The evaluated laser damage threshold value of the 2A5CTFA crystal is found to be 1.05GW/cm^2 and compared with some of the known organic NLO crystals in Table 3. Hence, from this analysis it is concluded that the 2-amino-5-chloropyridinium-trifluoroacetate crystal can withstand high intensity laser beams up to 1.05GW/cm^2.

Table 3 — LDT value of 2A5CTFA with other prominent NLO material

Compounds	LDT Values (GW/cm²)	References
KDP	0.2	[45]
Ammonium hydrogen L-tartrate	0.5	[46]
ISPA	0.22	[47]
$LiNbO_3$	0.3	[48]
2-methyl-4-nitroaniline	0.2	[49]
2A5CTFA	1.05	Present Work

4.6 Dielectric studies

The fundamental electrical properties of crystals can be understood by dielectric measurements. These are generally important to corelate the crystal electro-optic properties[50]. The dielectric investigation gives insight into the material properties with respect to the important parameters regarding structual, defect behaviour and diverse polarisation mechanisms[51-52]. The parallel plate capacitor formed by a clear 2A5CTFA single crystal placed between two nickel electrodes and encrusted with high-grade silver paste equally on both surfaces for good ohmic contact was used for the dielectric measurements. The capacitance accros the sample 2-Amino-5-Chloropyridinium trifluoroacetate crystal was determined at temperatures ranging from 308 to 348 K with frequencies ranging from 50 Hz to 5 MHz. The values of dielectric constant (ε') and dielectric loss (ε'') was determined by using the relations,

$$\varepsilon' = C_p d / A\varepsilon_0 \quad \ldots (4)$$

$$\varepsilon'' = \varepsilon' \tan\delta \quad \ldots (5)$$

Where 'C_p' is the parallel capacitance, 'd' is the thickness, 'A' is the area of cross-section and 'tanδ' is the dissipation factor. The variation of dielectric constant and dielectric loss with respective to varying frequency and temperature is shown in Fig. 7 and 8 respectively. It is observed from the graph that both the dielectric constant (ε') and the dielectric loss (ε'') values are comparatively high at a lower frequency and very low and insignificant at a higher frequencies. The presence of all polarisation mechanisms in the compound, namely space-charge, orientation, ionic and electronic polarisation is the reason for the large value of dielectric constants at higher frequencies. Furthermore, the low dielectric constant and dielectric

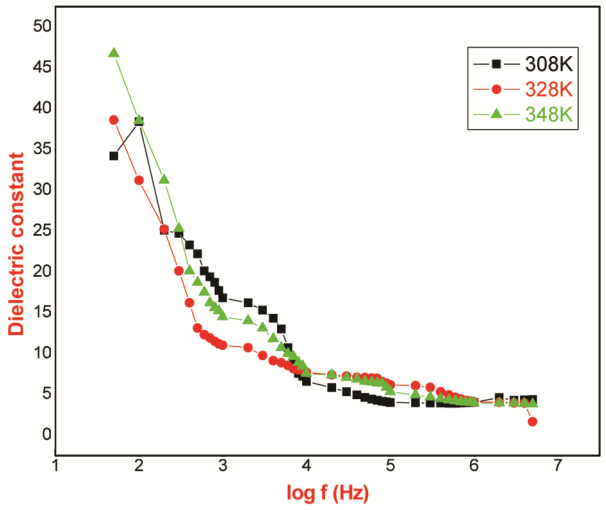

Fig. 7 — The variation of dielectric constant with log frequency of 2A5CTFA crystal

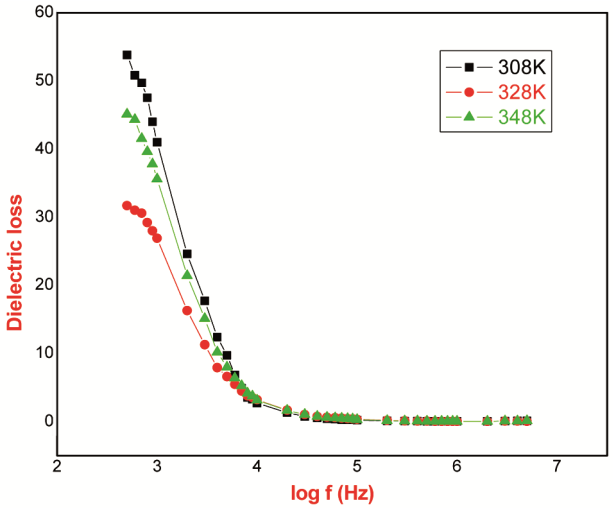

Fig. 8 — The variation of dielectric loss with log frequency of 2A5CTFA crystal

loss at higher frequencies reveals the normal optical behaviour of 2A5CTFA crystal. The enhanced optical quality of the crystal ensure its applications in microelectronics, photonics, lasers and electro-optic devices.

4.7 Estimation of solid-state parameters

The polarizability (α) is the significant parameter for the desired efficiency of the nonlinear optical effects[53]. The polarizability (α) of 2A5CTFA crystal was computed using the value of dielectric constant (ε_r) at higher frequency region. The required parameter, the density of the grown 2A5CTFA crystal is calculated from the X-ray diffraction data using the relation,

$$\rho = \frac{MZ}{N_a V} \quad \ldots (6)$$

Where 'M' denotes the Molecular weight (242.59g/mol) of the 2A5CTFA crystal, 'Z' is the number of molecules in the unit cell (Z=4), 'N_A' indicates the Avogadro's number (6.023×10^{23} mol^{-1}) and 'V' is the volume of the unit cell ($0.983\times10^{-21}cm^3$). The calculated density of the 2A5CTFA crystal 1.6391 g/cm^3 is well matches with the experimental value (1.615 g/cm^3) reported by single-crystal XRD analysis[26]. The valence electron plasma energy ($\hbar\omega_p$) is given by the relation[54],

$$\hbar\omega_p = 28.8\sqrt{(Z\rho/M)} \quad \ldots (7)$$

The calculated value of plasma energy ($\hbar\omega_p$) of the crystal is found to be 16.3464 eV. The Penn gap (E_p) and Fermi energy (E_F) of 2A5CTFA crystal in terms of plasma energy ($\hbar\omega_p$) was evaluated by using the following relations[55],

$$E_p = (\hbar\omega_p) / (\varepsilon_r\text{-}1)^{1/2} \quad \ldots (8)$$

Where, ε_r = 46.7 is the maximum value of dielectric constant of the material.

$$E_F = 0.2948\ (\hbar\omega_p)^{4/3} \quad \ldots (9)$$

The calculated values of Penn gap and Fermi energy using above equations (8) and (9) were summarised as 2.4180 and 12.2287 eV respectively.

Further, the polarizability (α) of the grown 2A5CTFA crystal was calculated by using the equation[56],

$$\alpha = \frac{0.396M}{\rho}\left[\frac{(\hbar\omega_p)^2 S_o}{(\hbar\omega_p)^2 S_o + 3E_p^2}\right] \times 10^{-24}\ cm^3 \quad \ldots (10)$$

Where, S_0 is the constant and the value of S_0 is obtained by using the following relation,

$$S_0 = 1\text{-}\left[\frac{E_p}{4E_f}\right] + \frac{1}{3}\left[\frac{E_p}{4E_f}\right]^2 \quad \ldots (11)$$

The calculated value of the constant S_0 = 0.9514. The polarizability (α) was calculated by using Clausius-Mossotti relation,

$$\alpha = \frac{3M}{4\pi N_a \rho}\left[\frac{\varepsilon_r - 1}{\varepsilon_r + 2}\right] cm^3 \quad \ldots (12)$$

The value of polarizability (α) was determined in terms of optical band gap E_g by using the expression,

$$\alpha = 0.396\left[1\text{-}\frac{\sqrt{Eg}}{4.06}\right]\frac{M}{\rho} \times 10^{-24}\ cm^3 \quad \ldots (13)$$

Table 4 — Calculated Solid-State parameters of the grown 2A5CTFA compound

Solid state parameters	Estimated values
Crystal density (ρ)	1.6391 g/cm^3 (Theoretical) 1.615 g/cm^3(Experimental)
Plasma energy ($h\omega_p$)	16.3464 (eV)
Penn gap energy (E_p)	2.4180 (eV)
Fermi energy (E_f)	12.2287 (eV)
Specific material constant (S_0)	0.9514
Electronic polarizability using Penn analysis (α)	5.4820X 10^{-23}(cm^3)
Electronic polarizability using Clausius-Mossotti (α)	5.5078 X 10^{-23}(cm^3)
Electronic polarizability using linear refractive index (α)	2.3914 X 10^{-23}(cm^3)
Electronic polarizability using optical band gap value (α)	3.1448 X 10^{-23}(cm^3)

The expression connecting the electronic polarization (α) and linear refractive index (μ) is given by the Lorentz-Lorentz equation as,

$$\alpha = \frac{3M}{4\pi N_a \rho}\left[\frac{\mu^2-1}{\mu^2+2}\right] \text{ cm}^3 \quad \ldots (14)$$

The calculated values of polarizabilities using above equations (10), (12), (13) and (14) are 5.4820×10^{-23}, 5.5078×10^{-23}, 3.1448×10^{-23} and 2.3914×10^{-23} cm^3 respectively. The obtained solid parameters of the grown 2-Amino-5-Chloropyridinium trifluoroacetate crystal are presented in Table 4.

4.8 Photoluminescence studies

Photoluminescence (PL) analysis is an non-destructive spectroscopic method in which a material is irradiated with light and the resulting spectrum is recorded as a plot of emitted light intensity versus wavelength. It finds wide application in various fields for analyzing organic compounds such as medical, chemical and bio-chemical research[57]. The emission spectrum of the grown 2A5CTFA obtained between 300 to 700 nm with the excitation wavelength 355 nm is depicted in Fig. 9. Examination of the spectrum gives violet fluorescence emission from 2A5CTFA crystal with the concentrated peak at 388 nm. The enhanced interaction of the COO^- group of trifluoroacetate with the lattice arrangement is testified by the prolongation of the emission peak up to 650 nm. The fluorescence emission peaks of the crystal shows good optical quality with the coverage of electronic transition in the entire band gap. The strong violet fluorescence emission peak confirms that the 2-amino-5-chloropyridinium-trifluoroacetate crystal is an suitable material for OLED device fabrications.

4.9 NLO property study

Using the Kurtz-Perry powder technique, the NLO efficiency of the powdered 2A5CTFA sample was investigated[58]. The fundamental laser light from a

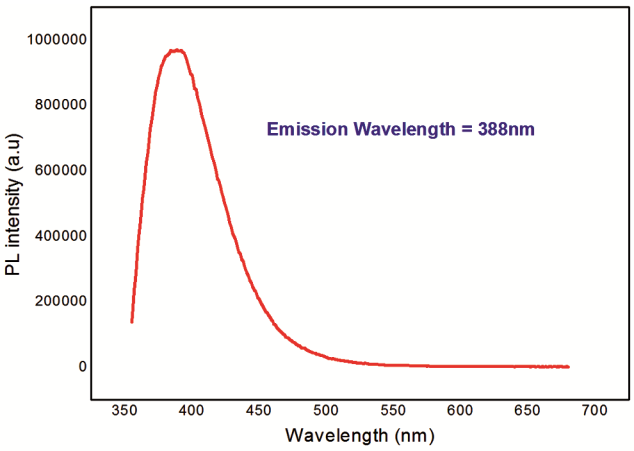

Fig. 9 — Photoluminescence spectrum of 2A5CTFA

Q-switched Nd: YAG laser with pulse energy of 6.05 mJ at 1064 nm, a recurrence rate of 10 Hz and a pulse width of 10 ns was used allowed to fall on the powdered sample. The output signal from the crystal is detected by the photomultiplier tube and displayed on the oscilloscope. Analysis of the output confirms the emission of green signal from the crystal at 532 nm, which confirms the second harmonic generation property. Hence this material can be used for frequency conversion and parametric oscillators. The reference material used for the study of 2A5CTFA sample was a powdered potassium dihydrogen phosphate (KDP) sample. In comparison, the 2A5CTFA crystal SHG efficiency was found to be 0.29 times that of KDP.

5 Conclusion

The organic nonlinear optical 2-amino-5-chloropyridinium-trifluoroacetate crystal was successfully grown at ambient temperature using methanol as solvent. Single crystal X-ray diffraction inferred that the 2-amino-5-chloropyridinium-trifluoroacetate crystal belongs to monoclinic system with space group P_c. The presence of various functional groups of 2A5CTFA crystal was confirmed by FTIR and FT-RAMAN analysis. The UV-Visible

transmission spectrum of the 2A5CTFA crystal reveals 85 percent transparency in the whole ultra-violet-visible region, with a lower cut-off wavelength of 345 nm. Thermal studies bringsforth that the 2-amino-5-chloropyridinium-trifluoroacetate crystal was stable up to 137^{o} C . The Photo luminescence behaviour of 2A5CTFA crystal has a violet emission radiation at 388 nm. The low dielectric constant and dielectric loss at higher frequency suggest that this crystal is of well optical quality for device applications. The SHG efficiency of 2A5CTFA is found to be comparable to that of ordinary KDP crystal. The LDT value of the 2A5CTFA compound was evaluated as 1.05 GW/cm^2 for 1064 nm wavelength of Nd: YAG laser. The above reasonable characterization results indicates that the grown 2-amino-5-chloropyridinium trifluoroacetate crystal can be used in the fabrication of optoelectronic and photonic devices.

Acknowledgments

The authors thank the authorities of SAIF, IIT Madras, Chennai-36, for completing the characterization such as Single Crystal XRD, FT-IR, FT-RAMAN and Thermal measurements.

References

1 Kanagasekaran T, Mythili P, Srinivasan P, Sharma S N & Gopalakrishnan R, *Mater Lett*, 62 (2008) 2486.
2 Helen F & Kanchana G, *Indian J Pure Appl Phys*, 52 (2014) 821.
3 Uma B, Selvaraj R S, Krishnan S & Boaz B M, *Optik*, 125 (2014) 651.
4 Nagapandiselvi P, Baby C & Gopalakrishnan R, *Rsc Adv*, 4 (2014) 22350.
5 Chemla D S & Zyss J, *Nonlinear optical properties of organic molecules and crystals*, Academic press, New York, 1 (1987) 448.
6 Babu B, Chandrasekaran J, Mohanbabu B, Matsushita Y & Saravanakumar M, *RSC Adv*, 6 (2016) 110884.
7 Sivasubramani V, Mohankumar V, Pandian M S & Ramasamy P, *Cryst Eng Commun*, 19 (2017) 5662.
8 Kvick A, Thomas R & Loetzle T F, *Acta Cryst*, B32 (1976) 224.
9 Zhang Y, Li H, Xi B, Che Y & Zheng J, *Mater Chem Phys*, 108 (2008) 192.
10 Dhanaraj P V, Rajesh N P & Bhagavannarayana G, *Phys-B Condensed Matter*, 405 (2010) 3441.
11 Pattison F L M, *Toxic Aliphatic Fluorine Compounds*, Elsevier Publishing Co, New York, 1959.
12 Trifluoracetic Acid Brochure, Halocarbon Products Corp. Hackensack, 11 (1967) 173. https://halocarbon.com/wp-content/uploads/2020/12/TFA-PSS-rev1-02162016.pdf
13 Jovita J V, Ramanand A, Sagayaraj P, Boopathi K & Ramasamy P, *Optik*, 126 (2014) 265.
14 Saravanakumar M, Chandrasekaran J, Krishnakumar M, Babu B, Vinitha G & Anis M, *J Phys Chem Sol*, 136 (2020) 109133.
15 Prasanyaa T, Haris M, Mathivanan V, Senthilkumar M, Mahalingam T, Jayaramakrishnan V, *Mater Chem Phys*, 147 (2014) 433.
16 Sun Z H, Zhang G H, Wang X Q, Yu G, Zhu L Y, Fan H L & Xu D, *J Cryst Growth*, 311 (2009) 3455.
17 Jayanalinaa T, Rajarajan G, Boopathi K & Sreevani K, *J Cryst Growth*, 426 (2015) 9.
18 Krishnakumar M, Karthick S, Thirupugalmani K & Brahadeeswaran S, *Opt Mater*, 66 (2017) 79.
19 Krishnakumar M, Thirupugalmani K & Brahadeeswaran S, *Mater Sci Poland*, (2017) 313.
20 Thanigaimani K, Khalib N C, Temel E, Arshad S & Razak I A, *J Mol Struct*, 1099 (2015) 246.
21 Suthan T, Rajesh N P, Mahadevan C K & Bhagavannarayana G, *Mater Chem Phys*, 129 (2011) 433.
22 Renugadevi R & Kesavaswamy R, Growth and characterization of 2-amino-5-chloropyridinium-trichloroacetate: A novel nonlinear optical single crystal, Taylor and francis, 88 (2015) 877.
23 Hemamalini M & Fun H K, *Acta Crystal*, E66 (2010) o557.
24 Jayanalinaa T, Rajarajan G, Boopathi K & Sreevani K, *J Cryst Growth*, 426 (2015) 9.
25 Hemamalini M & Fun H K, *Acta Crystal*, E66 (2010) o1416.
26 Hemamalini M & Fun H K, *Acta Cryst*, E66 (2010) o783.
27 Rao C N R, Ultra-Violet and Visible Spectroscopy: Chemical Applications, 3rd Edn, Butterworths, London, UK, (1975).
28 Chandran S K, Paulraj R & Ramasamy P, *J Cryst Growth*, 468 (2017) 68.
29 Boopathi K, Babu S M, Jagan R & Ramasamy P, *J Phys Chem Sol*, 111 (2017) 419.
30 Gomathi R & Madeswaran S, *Mater Chem Phys*, 218 (2018) 189.
31 Bhuvaneswari R, Bharathi M D, Anbalagan G & Murugesan K S, *Opt Mater*, 84 (2018) 728.
32 Hameed A S H, Ravi G, Dhanasekaran R & Ramasamy P, *J Cryst Growth*, 212 (2000) 227.
33 Priyadharshini A & Kalainathan S, *Opt Mater*, 78 (2018) 35.
34 Subhashini V, Ponnusamy S & Muthamizhchelvan C, *Acta Part A*, 87 (2012) 265.
35 Rajeswari A, Vinitha G & Murugakoothan P, *J Mater Sci Mater Electron*, 29 (2018) 12526.
36 Jeyaram J, Varadharajan K, Singaram B & Rajendhran R, *J Cryst Growth*, 486 (2018) 96.
37 Vimalan M, Kumar T R, Tamilselvan S, Sagayaraj P & Mahadevan C K, *Phys B*, 405 (2010) 3907.
38 Kutty P M, Chandrasekaran J, Babu B & Matsushita Y, *Z Phys Chem*, (2017) 802.
39 Suthan T, Rajesh N P, Mahadevan C K & Bhagavannarayana G, *Mater Chem Phys,* 129 (2011) 433.
40 Babu B, Chandrasekaran J, Mohanbabu B, Matsushita Y & Saravanakumar M, *RSC Adv*, 6 (2016) 110884.
41 Karthick S, Thirupugalmani K, Krishnakumar M, Kannan V, Vinitha G & Brahadeeswaran S, *Opt Laser Technol*, 122 (2020) 105849.
42 Bhat H L, *Bull Mater Sci*, 7 (1994) 1233.
43 Hanumantharao R, Kalainathan S, Bhagavannarayana G & Madhusoodanan U, *Acta Mol Biomol Spectrosc*, 103 (2013) 388.
44 Peramaiyan G, Pandi P, Vijayan N, Bhagavannarayana G & Kumar R M, J *Cryst Growth*, 375 (2013) 6.
45 Bhat H L, *Bull Mater Sci*, 7 (1994) 1233.

46 Hanumantharao R, Kalainathan S, Bhagavannarayana G & Madhusoodanan U, *Acta Mol Biomol Spectrosc*, 103 (2013) 388.
47 Jauhar R M, Viswanathan V, Vivek P, Vinitha G, Velmurugan D & Murugakoothan P, RSC Adv, 6 (2016) 57977.
48 Bhat H L, *Bull Mater Sci*, 17 (1994) 1233.
49 Takahashi Y, Onduka S, Brahadeeswaran S, Yoshimura M, Mori Y & Sasaki T, *Opt Mater*, 30 (2007) 116.
50 Boomadevi S & Dhanasekaran R, *J Cryst Growth*, 261 (2004) 70.
51 Mathew V, Jacob S, Mahadevan C K & Abraham K E, *Phys B*, 407 (2012) 222.
52 Babu B, Chandrasekaran J, Mohanbabu B, Matsushita Y & Saravanakumar M, *RSC Adv*, 6 (2016) 110884.
53 Jackson J D, Classical Electrodynamics, 2nd Edn, Wiley Eastern Limited, New York, (1978).
54 Ravindra N M, Bharadwaj R P, Sunil K K & Srivastava V K, *Infra Phys*, 21 (1981) 369.
55 Penn D R, *Phys Rev*, 128 (1962) 2093.
56 Born M, Wolf E, Osnovy Optiki 2nd Edn. Nauka, Moscow, (1970).
57 Lei J, Hou C, Huo D, Li Y, Luo X, Yang M, Fa H, Bao M, Li J & Deng B, *Atmos Pollut Res*, 7 (2016) 431.
58 Kurtz S K & Perry T T, *J Appl Phys*, 39 (1968) 3798.